Article ID: 1006-8775(2012) 01-0089-09

EFFECTS OF SEA SURFACE TEMPERATURE AND ITS DIURNAL VARIATION ON DIURNAL VARIATION OF RAINFALL: A PARTITIONING ANALYSIS BASED ON SURFACE RAINFALL BUDGET

CUI Xiao-peng (崔晓鹏)[1], Xiaofan LI (李小凡)[2]

(1. Laboratory of Cloud-Precipitation Physics and Severe Storms (LACS), Institute of Atmospheric Physics, Chinese Academy of Sciences, Beijing 100029 China; 2. NOAA/NESDIS/Office of Research and Applications, Camp Springs, Maryland, USA)

Abstract: The effects of sea surface temperature (SST) and its diurnal variation on diurnal variation of rainfall are examined in this study by analyzing a series of equilibrium cloud-resolving model experiments which are imposed with zero large-scale vertical velocity. The grid rainfall simulation data are categorized into eight rainfall types based on rainfall processes including water vapor convergence/divergence, local atmospheric drying/moistening, and hydrometeor loss/convergence or gain/divergence. The rainfall contributions of the rainfall types with water vapor convergence are insensitive to the increase in SST from 27°C to 29°C during the nighttime, whereas they are decreased during the daytime. The rainfall contributions of the rainfall types with water vapor convergence are decreased as the SST increases from 29°C to 31°C but the decreases are larger during the nighttime than during the daytime. The rainfall contributions of the rainfall types with water vapor convergence are decreased by the inclusion of diurnal variation of SST with diurnal difference of 1°C during the nighttime, but the decreases are significantly slowed down as the diurnal difference of SST increases from 1°C to 2°C. The rainfall contributions of the rainfall types with water vapor convergence are insensitive to the inclusion of diurnal variation of SST during the daytime.

Key words: sea surface temperature; diurnal variation; diurnal variation of rainfall; surface rainfall budget

CLC number: P435 **Document code:** A **doi:** 10.3969/j.issn.1006-8775.2012.01.010

1 INTRODUCTION

As one of the most important temporal variabilities, the diurnal cycle of rainfall has been intensively debated observationally and numerically for several decades[1-9]. The previous studies of diurnal variation of rainfall have been focused on the relationships between radiative cooling and nocturnal rainfall peak and between solar heating and daytime rainfall minimum. Recently, Cui[10] carried out diurnal analysis of surface rainfall budget and revealed that higher convective rain rate is associated with more water vapor convergence and higher stratiform rain rate is related to more water vapor convergence and more local atmospheric drying during the nighttime than during the daytime. Cui and Li[11] examined the effects of diurnal variation of imposed sea surface temperature (SST) on diurnal variation of convective and stratiform rainfall and showed that high SST in the afternoon transports a large amount of water vapor from rainfall-free regions to convective regions that increases afternoon rainfall.

Gao et al.[12] derived a diagnostic surface rainfall equation and revealed important contributions of water vapor and cloud processes to precipitation. Cui[13] categorized cloud-resolving model domain mean data into nine types (eight rainfall types and one rainfall-free type) and showed that while the water vapor convergence associated with large-scale ascending motions plays important roles in producing precipitation, the precipitation could occur in other environmental conditions such as large-scale water vapor divergence. Shen et al.[14] found that the local changes in water vapor and cloud hydrometeor concentration could be as important as the water vapor convergence in producing precipitation. The model domain mean, convective, and stratiform

Received 2010-12-20; **Revised** 2011-12-16; **Accepted** 2012-01-15

Foundation item: National Basic Research Program of China (973 Program) (2009CB421505); National Natural Sciences Foundation of China (40921160379, 40775036)

Biography: CUI Xiao-peng, Ph.D., professor of meteorology, mainly undertaking the research on mesoscale dynamics, mesoscale and cloud-scale numerical simulations, and surface rainfall processes.

Corresponding author: CUI Xiao-peng, e-mail: xpcui@mail.iap.ac.cn

rainfall only display averaged characteristics of rainfall, while containing different rainfall processes from each grid such as local atmospheric drying/moistening, water vapor convergence/divergence, and hydrometeor loss/convergence or gain/divergence. Shen et al.[15] studied precipitation statistics by categorizing grid rainfall model simulation data during a selected 21-day period of Tropical Ocean Global Atmosphere Coupled Ocean Atmosphere Response Experiment (TOGA COARE) into eight rainfall types and found that the rainfall with water vapor divergence and local atmospheric drying and hydrometeor loss/convergence has the largest contribution to total rainfall, while previous studies (e.g., Cui and Li[16]) revealed that convective rainfall contributes more to total rainfall than stratiform rainfall does. They further showed that a significant amount of convective rainfall comes from the regions with water vapor divergence, which contradicts the fact that convective rainfall is generally associated with water vapor convergence. Sensitivity of diurnal variations of convective and stratiform rainfall to SST and its diurnal variation were studied in Cui[10] and Cui and Li[11]. Effects of SST and its diurnal effects on diurnal variation of the eight tropical rainfall types[13-14] are investigated through a partitioning analysis of equilibrium sensitivity cloud-resolving model simulation data from Gao et al.[17] based on surface rainfall budget in this study. The model and experiments are briefly described in the next section. The results will be presented in section 3. The summary is given in section 4.

2 MODEL AND EXPERIMENTS

The simulation data analyzed in this study are from Gao et al.[17]. The cloud-resolving model used in Gao et al.[17] is a two-dimensional (2D) version of the model used by Sui et al.[7, 18] and further modified by Li et al.[19]. The model was originally developed by Soong and Ogura[20], Soong and Tao[21], and Tao and Simpson[22]. The model has cyclic lateral boundaries and includes prognostic equations for potential temperature, specific humidity, and perturbation momentum, in which the solar and thermal infrared radiation are parameterized by Chou et al.[23, 24] and Chou and Suarez[25]. The model uses five prognostic equations for the mixing ratios of cloud water, raindrops, cloud ice, snow, and graupel, whose cloud sources and sinks are parameterized by Lin et al.[26], Rutledge and Hobbs[27-28], Tao et al.[29] and Krueger et al.[30]. The model uses a horizontal domain of 768 km, horizontal grid resolution of 1.5 km, 33 vertical levels, and a time step of 12 s. The detailed model descriptions can be found in Gao and Li[31].

Experiments SST29, SST27 and SST31 are forced by time-invariant SSTs of 29, 27 and 31°C, respectively. Experiments SST29D1 and SST29D2 have diurnally-varying SSTs with a time mean of 29°C and diurnal difference of 1°C and 2°C, respectively. SST reaches maximum and minimum, respectively at hours 16 and 7 (Figure 1 in Gao et al.[17]). These five experiments were conducted by Gao et al.[17], which were integrated for 40 days with the 2D cloud-resolving model with a time and height invariant zonal wind, and zero large-scale vertical velocity. The vertical profiles of initial temperature and specific humidity were from the observations at 156°E and 1.75°S during TOGA COARE at 0400 LST 19 December 1992[6].

Following Gao et al.[12] and Cui and Li[16], the surface rainfall equation can be written as

$$P_s = Q_{WVT} + Q_{WVF} + Q_{WVE} + Q_{CM}, \quad (1)$$

$$Q_{WVT} = -\frac{\partial [q_v]}{\partial t}, \quad (1a)$$

$$Q_{WVF}$$

$$= -[\bar{u}^o \frac{\partial \bar{q}_v}{\partial x}] - [\frac{\partial (u' q_v')}{\partial x}] - [\bar{u}^o \frac{\partial q_v'}{\partial x}] - [w' \frac{\partial \bar{q}_v}{\partial z}], \quad (1b)$$

$$Q_{WVE} = E_s, \quad (1c)$$

$$Q_{CM} = Q_{CMC} + Q_{CMR} + Q_{CMI} + Q_{CMS} + Q_{CMG}, \quad (1d)$$

$$Q_{CMC} = -\frac{\partial [q_c]}{\partial t} - [\frac{\partial}{\partial x}(\bar{u}^o + u')q_c], \quad (2a)$$

$$Q_{CMR} = -\frac{\partial [q_r]}{\partial t} - [\frac{\partial}{\partial x}(\bar{u}^o + u')q_r], \quad (2b)$$

$$Q_{CMI} = -\frac{\partial [q_i]}{\partial t} - [\frac{\partial}{\partial x}(\bar{u}^o + u')q_i], \quad (2c)$$

$$Q_{CMS} = -\frac{\partial [q_s]}{\partial t} - [\frac{\partial}{\partial x}(\bar{u}^o + u')q_s], \quad (2d)$$

Here u and w are zonal and vertical components of wind, respectively; q_c, q_r, q_i, q_s, q_g are the mixing ratios of cloud water, raindrops, cloud ice, snow, and graupel, respectively; $\bar{u}^o$ =4 m s^{-1}; the overbar denotes a model domain-mean; a prime denotes a perturbation from the model domain mean; and the symbol ° is an imposed forcing; mass integration $[()] = \int_{z_b}^{z_t} \bar{\rho}() dz$, and z_t and z_b are the heights of the top and bottom of the model

atmosphere, respectively. The surface rainfall budget (1) states that the surface rain rate (P_S) is determined by local atmospheric moistening (Q_{WVT} <0)/drying (Q_{WVT} >0), water vapor convergence (Q_{WVF} >0)/divergence (Q_{WVF} <0), surface evaporation (Q_{WVE}), and decrease of local hydrometeor concentration/hydrometeor convergence (Q_{CM} >0) or increase of local hydrometeor concentration/hydrometeor divergence (Q_{CM} <0). Following Cui[13] and Shen et al.[15], eight rainfall types (TFM, TFm, tFM, tFm, TfM, Tfm, tfM, and tfm) will be categorized using the grid simulation data based on different signs of Q_{WVF}, Q_{WVT}, and Q_{CM} (see the summary of rainfall types in Table 1), where T and t represent local atmospheric drying (Q_{WVT} >0) and moistening (Q_{WVT} <0), respectively. F and f denote water vapor convergence (Q_{WVF} >0) and divergence (Q_{WVF} <0), respectively. M and m represent hydrometeor loss/convergence (Q_{CM} >0) and hydrometeor gain/divergence (Q_{CM} <0), respectively. tfm will not be analyzed in this study because it has very small rainfall. The fractional rainfall coverage (FRC) of each rainfall type is calculated by dividing the grids for each rainfall type over total rainfall grid. The rainfall contribution of each rainfall type is calculated by dividing the rainfall from each type over total rainfall (PRA). The radiation is a key process responsible for the diurnal variation of rainfall. The solar radiative heating is larger than the infrared (IR) radiative cooling during the daytime from hour 7 to hour 18, which leads to radiative heating. The solar radiative heating is absent during the nighttime from hour 19 to midnight and from midnight to hour 6, so the IR cooling determines the radiative cooling. Thus, surface rain rates during the nighttime and daytime are calculated using the grid rainfall simulation data, respectively, from hour 19 to hour 6 and from hour 7 to hour 18. The hourly instantaneous grid data from day 21 to 40 are analyzed in the following discussions.

Table 1. Summary of rainfall types. T and t represent local atmospheric drying and moistening, respectively. F and f represent water vapor convergence and divergence, respectively. M and m represent local atmospheric loss and gain, respectively.

Type	Description
TFM	Water vapor convergence, local atmospheric drying, and hydrometeor loss/convergence
TFm	Water vapor convergence, local atmospheric drying, and hydrometeor gain/divergence
tFM	Water vapor convergence, local atmospheric moistening, and hydrometeor loss/convergence
tFm	Water vapor convergence, local atmospheric moistening, and hydrometeor gain/divergence
TfM	Water vapor divergence, local atmospheric drying, and hydrometeor loss/convergence
Tfm	Water vapor divergence, local atmospheric drying, and hydrometeor gain/divergence
tfM	Water vapor divergence, local atmospheric moistening, and hydrometeor loss/convergence
tfm	Water vapor divergence, local atmospheric moistening, and hydrometeor gain/divergence

3 RESULTS

The analysis of the rainfall contribution measured by the PRA in SST29 shows that the rainfall with water vapor convergence (TFM+TFm+tFM+tFm) contribute more to total rainfall during the nighttime than during the daytime primarily due to the larger contribution of the rainfall type with local atmospheric drying and hydrometeor loss/convergence (TFM) during the nighttime (Table 2 and Figure 1). The mean surface rain rate of TFM is higher during the nighttime than during the daytime, which results from the larger water vapor convergence, local atmospheric drying, and hydrometeor loss/convergence during the nighttime. The rain water hydrometeor loss/convergence is smaller but the cloud hydrometeor loss/convergence is larger during the nighttime than during the daytime. The graupel hydrometeor gain/divergence occurs during the daytime, whereas it is negligibly small during the nighttime. Thus, the increase in hydrometeor loss/convergence from the daytime to the nighttime in TFM is associated with the increase in cloud water hydrometeor loss/convergence and dramatic decrease in graupel hydrometeor gain/divergence. The rainfall contribution of the rainfall type with local atmospheric drying and hydrometeor loss/convergence (TfM), a largest contributor in the rainfall with water vapor divergence (TfM+Tfm+tfM), is smaller during the nighttime than during the daytime, which comes from the shrink of rainfall coverage (decrease in FRC) and the weakened surface rainfall from the daytime to the nighttime. The rainfall decrease from the daytime to the nighttime is related to the decreases in local atmospheric drying and water (cloud water and rain) hydrometeor loss/convergence.

Table 2. (a) Percentage of total rainfall amount from rainfall type (PRA) with water vapor convergence (TFM+TFm+tFM+tFm) during nighttime (NT) and daytime (DY) in the five experiments and (b) their differences for SST29-SST27, SST31-SST29, SST29D1-SST29, and SST29D2-SST29D1. Unit is %.

(a)	SST29	SST27	SST31	SST29D1	SST29D2
PRA.NT	76.4	76.5	72.9	74.2	75.6
PRA.DY	73.6	78.3	72.4	73.3	73.7

(b)	SST29–SST27	SST31–SST29	SST29D1SST29	SST29D2SST29D1
PRA.NT	–0.1	–3.5	–2.2	1.4
PRA.DY	–4.7	–1.2	–0.3	0.4

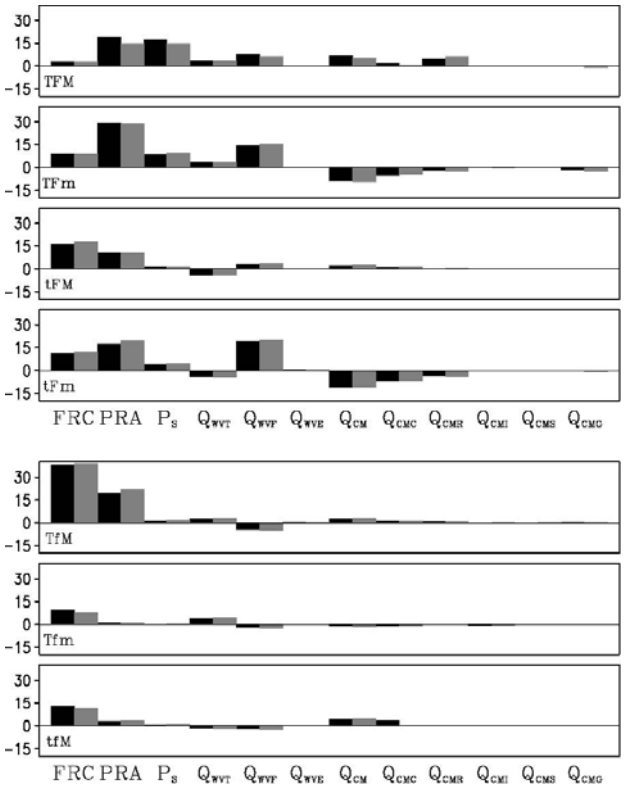

Figure 1. Fractional rainfall coverage (FRC) and percentage of rain amount over total rainfall amount (PRA), and means of P_S, Q_{WVT}, Q_{WVF}, Q_{WVE}, Q_{CM}, *QCMC*, *QCMR*, *QCMI*, *QCMS*, and *QCMG* of TFM, TFm, tFM, tFm, TfM, Tfm, and tfM during nighttime (black bar) and daytime (grey bar) in SST29. Units are mm h^{-1} for P_S, Q_{WVT}, Q_{WVF}, Q_{WVE}, and Q_{CM} and % for FRC and PRA.

When the time-invariant SST increases from 27°C in SST27 to 29°C in SST29, the rainfall contributions of the rainfall types with water vapor convergence are barely changed during the nighttime whereas they are decreased during the daytime (Table 2). During the nighttime, the similar rainfall contributions of the rainfall types with water vapor convergence in the two experiments result from the offset between the increase in rainfall contribution of the rainfall type(TFm) with local atmospheric drying and hydrometeor gain/divergence and the decrease in rainfall contribution of the rainfall type(tFm) with local atmospheric moistening and hydrometeor gain/divergence (Figure 2). The insensitivity of rainfall contributions of the rainfall types with water vapor divergence to the increase in SST results from the offset between the increase in rainfall contribution of TfM and the decreases in rainfall contributions of the rainfall types with local atmospheric drying and hydrometeor gain/divergence (Tfm) and with local atmospheric moistening and hydrometeor loss/convergence (tfM) in nighttime (Figure 2). In nighttime the increase in rainfall contribution of TfM corresponds to the expanded rainfall coverage and enhanced surface rainfall through the increases in local atmospheric drying and water hydrometeor loss/convergence, and the decreases in rainfall contributions of Tfm and tfM are related to the shrink of rainfall coverage. During the daytime, the decrease in rainfall contributions of the rainfall types with water vapor convergence caused by the increase in SST from 27°C to 29°C is mainly from the decreases in rainfall contributions of TFM and tFM through the shrink of rainfall coverage. The increase in rainfall contributions of the rainfall types with water vapor divergence results from the enhanced contribution of TfM through the expanded rainfall coverage and increased surface rainfall; the increased rainfall is associated with the increases in local atmospheric drying and water hydrometeor loss/convergence.

When the time-invariant SST increases from 29°C in SST29 to 31°C in SST31, the rainfall contributions of the rainfall types with water vapor convergence are decreased, but the decrease is larger during the nighttime than during the daytime (Table 2). During the nighttime, the contribution decrease is primarily from the decrease in rainfall contribution of TFM (Figure 3). The increase in rainfall contributions of the rainfall types with water vapor divergence is primarily from the increase in rainfall contribution of TfM through the expansion in rainfall coverage and the increase in surface rainfall. The rainfall enhancement

corresponds to the intensifications in local atmospheric drying and rain hydrometeor loss/convergence. During the daytime, the decrease in rainfall contribution of the rainfall types with water vapor convergence is primarily from the decreased rainfall contribution of tFm through the shrink of rainfall coverage. The increased rainfall contributions of the rainfall types with water vapor divergence caused by the increase in SST from 29 to 31°C are intimately associated with the enhanced rainfall contribution of TfM through the strengthened surface rainfall; it appears to be from the increases in local atmospheric drying and water hydrometeor loss/convergence.

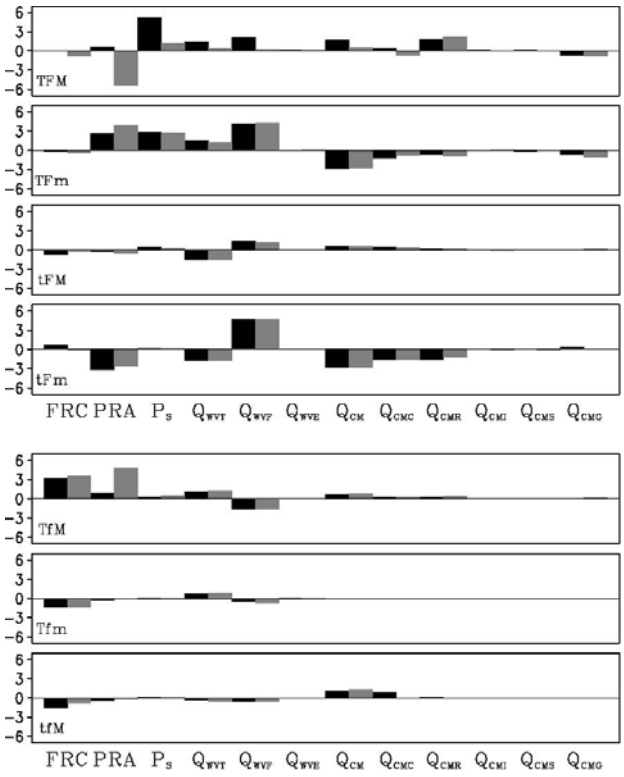

Figure 2. Fractional rainfall coverage (FRC) and percentage of rain amount over total rainfall amount (PRA), and means of P_S, Q_{WVT}, Q_{WVF}, Q_{WVE}, Q_{CM}, *QCMC*, *QCMR*, *QCMI*, *QCMS*, and *QCMG* of TFM, TFm, tFM, tFm, TfM, Tfm, and tfM during nighttime (black bar) and daytime (grey bar) for SST29-SST27. Units are mm h^{-1} for P_S, Q_{WVT}, Q_{WVF}, Q_{WVE}, and Q_{CM} and % for FRC and PRA.

When the time-invariant SST in SST29 is replaced with the diurnal variation of SST with the diurnal difference of 1°C in SST29D1, the rainfall contributions from the rainfall types with water vapor convergence are decreased during the nighttime whereas they are barely changed during the daytime (Table 2). During the nighttime, the decreased rainfall contribution results from the reductions in rainfall contributions of TFM and tFM through the shrink of rainfall coverage in TFM and tFM and the weakened surface rainfall in tFM due to the decrease in water vapor convergence and cloud water hydrometeor loss/convergence (Figure 4). The enhanced rainfall contributions of the rainfall types with water vapor divergence are primarily from the enhancement in rainfall contribution of TfM through the expansion of rainfall coverage. During the daytime, the insensitivity of rainfall contributions of the rainfall types with water vapor convergence to the diurnal variation of SST results from the large offset between the increased rainfall contribution of TFm and the decreased rainfall contribution of tFm. The increase in rainfall contribution of TFm comes from the strengthened surface rainfall through the intensifications in local atmospheric drying and water vapor convergence, whereas the decrease in rainfall contribution of tFm is caused by the shrink of rainfall coverage.

When the diurnal difference of 1°C in SST29D1 is replaced with 2°C in SST29D2, the rainfall contributions of the rainfall types with water vapor convergence are increased during the nighttime but they are barely varied during the daytime (Table 2). During the nighttime, the enhanced rainfall contributions are primarily from the increased rainfall contribution of tFM through the expanded rainfall coverage and strengthened surface rainfall associated with the increases in water vapor convergence and water hydrometeor loss/convergence (Figure 5). During the daytime, the similar rainfall contributions of the rainfall types with water vapor convergence in SST29D1 and SST29D2 result from the near offset between the increase in rainfall contribution of TFM and the decreases in rainfall contributions of TFm and tFM. The increased rainfall contribution of TFM comes from the increases in rainfall coverage and surface rainfall though the intensifications in water vapor convergence and local atmospheric drying and water hydrometeor loss/convergence. The reduced rainfall contributions come from the shrink of rainfall coverage in tFM and the weakening of surface rainfall through the slowdown in water vapor convergence in TFm.

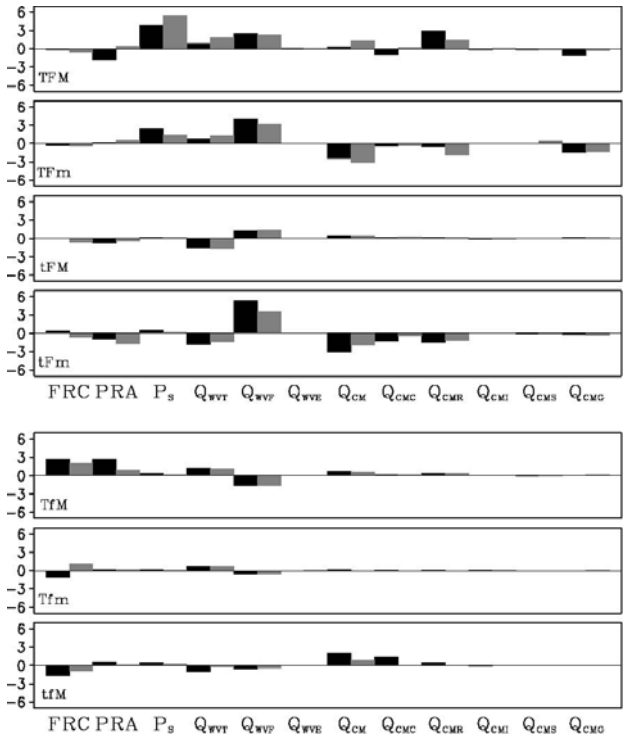

Figure 3. As in Figure 2 except for SST31-SST29.

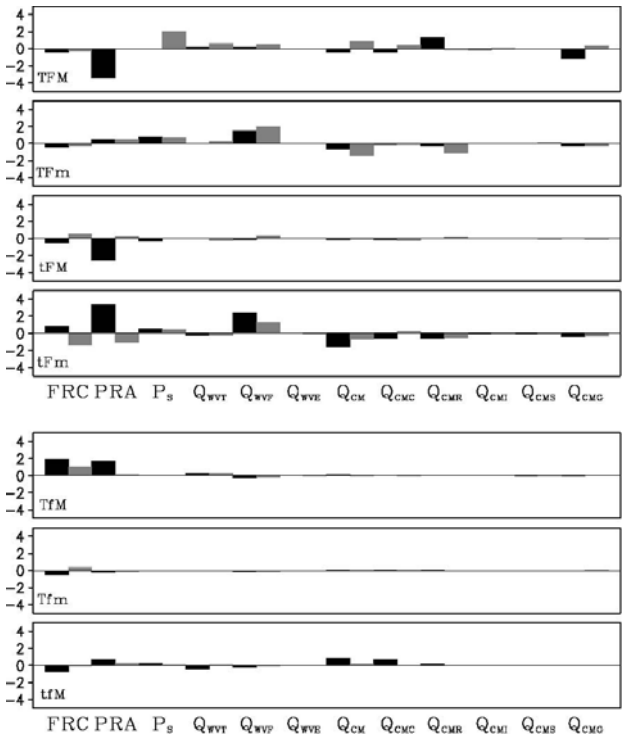

Figure 4. As in Figure 2 except for SST29D1-SST29.

Convective rainfall is usually associated with water vapor convergence. To examine differences in PRA between the rainfall with water vapor convergence in this study and convective rainfall in previous studies[10, 11], PRA of convective rainfall during the nighttime and daytime is calculated using the grid rainfall simulation data, respectively, from hour 19 to hour 6 and from hour 7 to hour 18 (Table 3). Convective rainfall is partitioned using the separation scheme developed by Tao et al.[32] and modified by Sui et al.[18]. The differences between this study (Table 2) and previous studies (Table 3) include the following: (1) the PRA of the rainfall with water vapor convergence in this study is significantly larger than that of convective rainfall; (2) during the nighttime, the increase in SST from 27°C to 29°C barely changes the PRA in this study but it decreases the PRA in previous studies; (3) the increase in SST from 29°C to 31°C decreases the PRA in this study whereas it increases the PRA in previous studies; (4) during the daytime, the decrease in PRA resulting from the diurnal variation of SST with the diurnal difference of 1°C and the increase in PRA caused by the diurnal variation of SST with the diurnal difference of 2°C are much smaller in this study than in previous studies.

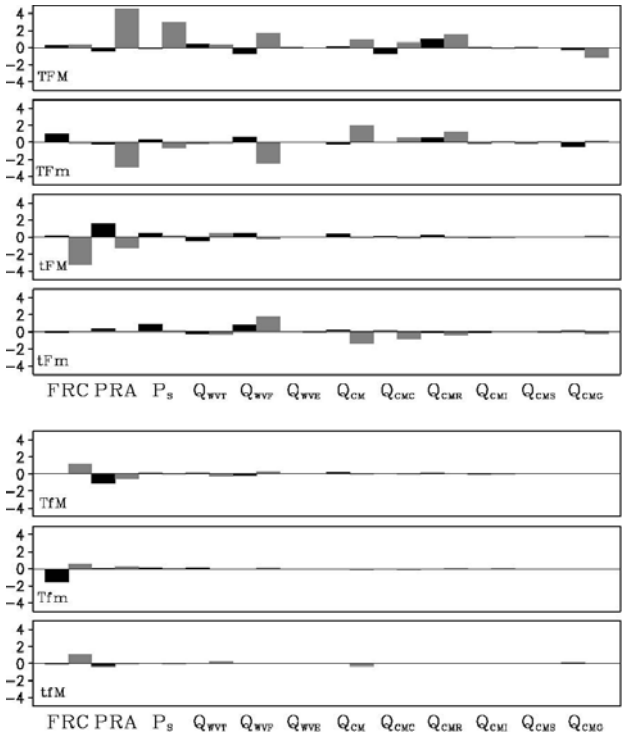

Figure 5. As in Figure 2 except for SST29D2-SST29D1.

Table 3. (a) Percentage of total rainfall amount from convective rainfall (PRA) during nighttime (NT) and daytime (DY) in the five experiments and (b) their differences for SST29-SST27, SST31-SST29, SST29D1-SST29, and SST29D2-SST29D1. Unit is %.

(a)	SST29	SST27	SST31	SST29D1	SST29D2
PRA.NT	58.0	56.4	62.3	60.2	60.3
PRA.DY	55.9	53.7	61.3	58.4	62.6

(b)	SST29–SST27	SST31–SST29	SST29D1SST29	SST29D2SST29D1
PRA.NT	–1.6	4.3	–2.1	2.3
PRA.DY	–2.2	5.4	–2.9	6.7

4 SUMMARY

The effects of SST and its diurnal variation on diurnal variations of rainfall are investigated by analyzing the equilibrium two-dimensional cloud-resolving simulation data from Gao et al.[17]. The experiments are imposed by zero large-scale vertical velocity and time and height invariant zonal wind in the model and integrated for about 40 days. The last 20-day equilibrium simulation data are used for the analysis. The surface rainfall equation proposed by Gao et al.[12] is used to categorize grid rainfall simulation data into eight types of rainfall, and the analysis of diurnal variation of rainfall is conducted for the nighttime from hour 19 to hour 6 and the daytime from hour 7 to hour 18. The major results include the following.

(1) The rainfall contributions of the rainfall types with water vapor convergence are decreased when the SST increases from 27°C to 29°C during the daytime or when the SST increases from 29°C to 31°C during the nighttime and daytime or when the diurnal variation of SST is included during the nighttime, but they are increased when the diurnal difference of SST increases from 1°C to 2°C during the nighttime. Otherwise, they are barely changed. The results reveal that although SST is increased by 2°C, the increases in SST from 27°C to 29°C and from 29°C to 31°C have different impacts on diurnal variations of rainfall. The diurnal variation of SST impacts rainfall contributions of the rainfall types with water vapor convergence during the nighttime but it almost does not have any effects during the daytime.

(2) The decreased rainfall contributions of the rainfall types with water vapor convergence are associated with the reduced rainfall contribution of the rainfall type(TFM) with local atmospheric drying and hydrometeor loss/convergence caused by the increase in SST from 27°C to 29°C during the daytime and by the increase in SST from 29°C to 31°C during the nighttime, and from the rainfall (tFm) with local atmospheric moistening and hydrometeor gain/divergence caused by the increase from 29°C to 31°C during the daytime through the shrink of rainfall coverage.

(3) The reduced rainfalls contributions of the rainfall types with water vapor convergence caused by the inclusion of diurnal variation of SST with the diurnal difference of 1°C during the nighttime correspond to the decrease in rainfall contributions of TFM and tFM through the shrink of rainfall coverage. The enhanced rainfall contributions of the rainfall types with water vapor convergence caused by the replacement of 1°C of the diurnal difference of SST with 2°C during the nighttime are primarily related to the increase in rainfall contribution of tFM through the expansion in rainfall coverage and intensification in surface rainfall.

Caution should be exercised here since only 2D simulation data with imposed zero large-scale vertical velocity and spatially uniform zonal wind are analyzed in this study. Further studies with 3D cloud-resolving models with imposed non-zero large-scale vertical velocity and spatially varying zonal wind and 3D interactive models are necessary to examine the effects of SST and its diurnal variation on diurnal variation of rainfall and to validate the 2D results from this study.

Acknowledgement: The authors thank Prof. GAO Shou-ting at the Institute of Atmospheric Physics, Chinese Academy of Sciences, Beijing, China for his equilibrium cloud-resolving simulation data.

REFERENCES:

[1] KRAUS E B. The diurnal precipitation change over the sea [J]. J. Atmos. Sci., 1963, 20(6): 546-551.
[2] GRAY W M, Jacobson R W. Diurnal variation of deep cumulus convection [J]. Mon. Wea. Rev., 1977, 105(9): 1171-1188.
[3] RANDALL D A, Harshvardhan, Dazlich D A.

Diurnal variability of the hydrologic cycle in a general circulation model [J]. J. Atmos. Sci., 1991, 48(1): 40-62.
[4] SUI C H, LAU K M. Multiscale phenomena in the tropical atmosphere over the western Pacific [J]. Mon. Wea. Rev., 1992, 120(3): 407-430.
[5] TAO W K, LANG S, SIMPSON J, et al. Mechanisms of cloud-radiation interaction in the tropics and midlatitudes [J]. J. Atmos. Sci., 1996, 53(18): 2624-2651.
[6] SUI C H, LAU K M, TAKAYABU Y N, et al. Diurnal variations in tropical oceanic cumulus convection during TOGA COARE [J]. J. Atmos. Sci., 1997, 54(5): 639-655.
[7] SUI C H, LI X F, LAU K M. Radiative-convective processes in simulated diurnal variations of tropical oceanic convection [J]. J. Atmos. Sci., 1998, 55(13): 2345-2357.
[8] LIU C, MONCRIEFF M W. A numerical study of the diurnal cycle of tropical oceanic convection [J]. J. Atmos. Sci., 1998, 55(13): 2329-2344.
[9] YANG S, KUO K S, SMITH E A. Persistent nature of secondary diurnal modes of precipitation over oceanic and continental regions [J]. J. Climate, 2008, 21(16): 4115-4131.
[10] CUI X P. A cloud-resolving modeling study of diurnal variations of tropical convective and stratiform rainfall [J]. J. Geophys. Res., 2008, 113, D02113, doi: 10.1029/2007JD008990.
[11] CUI X P, LI X F. Diurnal responses of tropical convective and stratiform rainfall to diurnally varying sea surface temperature [J]. Meteor. Atmos. Phys., 2009, 104(1): 53-61.
[12] GAO S T, CUI X P, ZHOU Y S et al. Surface rainfall processes as simulated in a cloud resolving model [J]. J. Geophys. Res., 2005, 110, D10202, doi: 10.1029/2004JD005467.
[13] CUI X P. Quantitative diagnostic analysis of surface rainfall processes by surface rainfall equation [J]. Chin. J. Atmos. Sci., 2009, 33(2): 375-387.
[14] SHEN X, WANG Y, ZHANG N et al. Roles of large-scale forcing, thermodynamics, and cloud microphysics in tropical precipitation processes [J]. Atmos.Res.,2010,doi:10.1016/j.atmosres.2010.04.014.
[15] SHEN X, WANG Y, ZHANG N et al. Precipitation and cloud statistics in the deep tropical convective regime [J]. J. Geophys. Res., 2010, 115, D24205, doi:10.1029/2010JD014481.
[16] CUI X P, LI X F. Role of surface evaporation in surface rainfall processes[J]. J. Geophys. Res., 2006, 111, D17112, doi:10.1029/2005JD006876.
[17] GAO S, ZHOU Y, Li X. Effects of diurnal variations on tropical equilibrium states: A two-dimensional cloud-resolving modeling study [J]. J. Atmos. Sci., 2007, 64(2): 656-664.
[18] SUI C H, LAU K M, TAO W K et al. The tropical water and energy cycles in a cumulus ensemble model. Part I: Equilibrium climate [J]. J. Atmos. Sci., 1994, 51(5): 711-728.
[19] LI X, SUI C H, LAU K M et al. Large-scale forcing and cloud-radiation interaction in the tropical deep convective regime [J]. J. Atmos. Sci., 1999, 56(17): 3028-3042.
[20] SOONG S T, OGURA Y. Response of tradewind cumuli to large-scale processes [J]. J. Atmos. Sci., 1980, 37(9): 2035-2050.
[21] SOONG S T, TAO W K. Response of deep tropical cumulus clouds to Mesoscale processes [J]. J. Atmos. Sci., 1980, 37(9): 2016-2034.
[22] TAO W K, SIMPSON J. The Goddard Cumulus Ensemble model. Part I: Model description [J]. Terr. Atmos. Oceanic Sci., 1993, 4(1): 35-72.
[23] CHOU M D, KRATZ D P, RIDGWAY W. Infrared radiation parameterization in numerical climate models [J]. J. Climate, 1991, 4(4): 424-437.
[24] CHOU M D, SUAREZ M J, HO C H, et al. Parameterizations for cloud overlapping and shortwave single scattering properties for use in general circulation and cloud ensemble models [J]. J. Climate, 1998, 11(2): 202-214.
[25] CHOU M D, SUAREZ M J. An efficient thermal infrared radiation parameterization for use in general circulation model [R]. NASA Tech. Memo. 1994, 104606, Vol. 3, 85pp. [Available from NASA/Goddard Space Flight Center, Code 913, Greenbelt, MD 20771.
[26] LIN Y L, FARLEY R D, ORVILLE H D. Bulk parameterization of the snow field in a cloud model [J]. J. Clim. Appl. Meteor., 1983, 22(6): 1065-1092.
[27] RUTLEDGE S A, HOBBS P V. The mesoscale and microscale structure and organization of clouds and precipitation in midlatitude cyclones. VIII: A model for the "seeder-feeder" process in warm-frontal rainbands [J]. J. Atmos. Sci., 1983, 40(5): 1185-1206.
[28] RUTLEDGE S A, HOBBS P V. The mesoscale and microscale structure and organization of clouds and precipitation in midlatitude cyclones. XII: A disgnostic modeling study of precipitation development in narrow cold-frontal rainbands [J]. J. Atmos. Sci., 1984, 41(20): 2949-2972.
[29] TAO W K, SIMPSON J, McCUMBER M. An ice-water saturation adjustment [J]. Mon. Wea. Rev., 1989, 117(1): 231-235.
[30] KRUEGER S K, FU Q, LIOU K N, et al. Improvement of an ice-phase microphysics parameterization for use in numerical simulations of tropical convection [J]. J. Appl. Meteor., 1995, 34(1): 281-287.
[31] GAO S T, LI X F. Cloud-resolving modeling of convective processes [M]. 2008, Dordrecht: Springer, 206pp.
[32] TAO W K, SIMPSON J, SUI C H, et al. Heating, moisture and water budgets of tropical and midlatitude squall lines: Comparisons and sensitivity to longwave radiation [J]. J. Atmos. Sci., 1993, 50(5): 673-690.

Citation: CUI Xiao-peng and Xiaofan LI. Effects of Sea Surface Temperature and its Diurnal Variation on Diurnal Variation of Rainfall: A Partitioning Analysis Based on Surface Rainfall Budget. J. Trop. Meteor., 2012, 18(1): 89-97.